J|A|C|S ARTICLES

Published on Web 08/06/2009

Exploring Photoreactions between Polyazaaromatic Ru(II) Complexes and Biomolecules by Chemically Induced Dynamic Nuclear Polarization Measurements

Sandrine Perrier,[†] Epiphanie Mugeniwabagara,[†] Andrée Kirsch-De Mesmaeker,[‡] P. J. Hore,[§] and Michel Luhmer*[,†]

Laboratoire de Résonance Magnétique Nucléaire Haute Résolution and Service de Chimie Organique et Photochimie CP 160/08, Université Libre de Bruxelles, 50 Av. F.D. Roosevelt, B-1050 Bruxelles, Belgium, Physical & Theoretical Chemistry Laboratory, Department of Chemistry, University of Oxford, South Parks Road, Oxford OX1 3QZ, U.K.

Received April 4, 2009; E-mail: michel.luhmer@ulb.ac.be

Abstract: Steady-state ^{1}H photo-chemically induced dynamic nuclear polarization (CIDNP) experiments were conducted at 14.1 T on deoxygenated (buffered pH 7) aqueous solutions of $[Ru(phen)_3]^{2+}$, $[Ru(tap)_2(phen)]^{2+}$, and $[Ru(tap)_3]^{2+}$ (tap = 1,4,5,8-tetraazaphenanthrene; phen = 1,10-phenanthroline) in the presence of guanosine-5′-monophosphate or *N*-acetyltyrosine. For the first time, CIDNP arising from photo-oxidation by polyazaaromatic Ru(II) complexes is reported. In agreement with the occurrence of a photo-electron-transfer process, photo-CIDNP effects are observed with $[Ru(tap)_3]^{2+}$ and $[Ru(tap)_2(phen)]^{2+}$ but not with $[Ru(phen)_3]^{2+}$. With $[Ru(tap)_2(phen)]^{2+}$, no significant photo-CIDNP is observed for the ^{1}H nuclei of the phen ligand, consistent with the fact that the metal-to-ligand charge-transfer triplet excited states responsible for the photo-oxidation involve a tap ligand. Successive experiments with $[Ru(tap)_3]^{2+}$ highlight the accumulation of long-lived radical species in solution that cause ^{1}H NMR signal broadening and photo-CIDNP extinction. The ^{1}H photo-CIDNP observed for the biomolecules is rather weak, less than about 30% of the equilibrium magnetization. However, up to 60% polarization enhancement is observed for H-2 and H-7 of the tap ligands, which indicates high unpaired electron density in the vicinity of these atoms in the transient radical pair. This is consistent with the structure of known photoadducts formed, for instance, between the metallic compounds and the guanine base of mono- and polynucleotides. Indeed, in these adducts the covalent bond involves carbon C-2 or C-7 of a tap ligand. The occurrence of photo-CIDNP with polyazaaromatic Ru(II) complexes opens new perspectives for the study of this type of compound.

Introduction

Polypyridyl Ru(II) complexes are characterized by a luminescence in the visible light spectrum that is highly sensitive to their local environment.[1−3] In addition, when they contain at least two polyazaaromatic 1,4,5,8-tetraazaphenanthrene (tap) or 1,4,5,8,9,12-hexaazatriphenylene (hat) ligands, they photo-oxidize some amino acids, such as tyrosine and tryptophan, and purine nucleobases (Chart 1).[4,5] It has also been demonstrated that the photoreactions of these polyazaaromatic Ru(II) complexes with tryptophan and the guanine base (in guanosine-5′-monophosphate or DNA) give rise to the formation of covalent adducts (Chart 1).[4,6,7] On the basis of these interesting properties, polyazaaromatic Ru(II) complexes are being developed as photoprobes of genetic material and as potential photoactive drugs in gene therapy.[8] Blue light absorption by these metallic compounds, followed by fast intersystem crossing, yields metal-to-ligand charge-transfer triplet excited (^{3}MLCT) states with a quantum yield close to unity (see Supporting Information).[9,10] The π-acceptor ligands tap and hat are common electron-accepting ligands of the lowest energy ^{3}MLCT states.[4,5] Owing to their long lifetime, typically between 10^{-7} and 10^{-6} s, and their highly oxidizing and reducing potentials, these ^{3}MLCT states are responsible for the remarkable properties of polyazaaromatic Ru(II) complexes. Various processes compete for the deactivation of the excited complex to the ground state. A

[†] Laboratoire de Résonance Magnétique Nucléaire Haute Résolution, Université Libre de Bruxelles.

[‡] Service de Chimie Organique et Photochimie, Université Libre de Bruxelles.

[§] University of Oxford.

(1) Friedman, A. E.; Chambron, J. C.; Sauvage, J. P.; Turro, N. J.; Barton, J. K. *J. Am. Chem. Soc.* **1990**, *112*, 4960–4962.
(2) Jenkins, Y.; Friedman, A. E.; Turro, N. J.; Barton, J. K. *Biochemistry* **1992**, *31*, 10809–10816.
(3) Olofsson, J.; Onfelt, B.; Lincoln, P.; Norden, B.; Matousek, P.; Parker, A. W.; Tuite, E. *J. Inorg. Biochem.* **2002**, *91*, 286–297.
(4) Elias, B.; Kirsch-De Mesmaeker, A. *Coord. Chem. Rev.* **2006**, *250*, 1627–1641.
(5) Herman, L.; Ghosh, S.; Defrancq, E.; Kirsch-De Mesmaeker, A. *J. Phys. Org. Chem.* **2008**, *21*, 670–681.
(6) Gicquel, E.; Boisdenghien, A.; Defrancq, E.; Moucheron, C.; Kirsch-De Mesmaeker, A. *Chem. Commun.* **2004**, 2764–2765.
(7) Blasius, R.; Nierengarten, H.; Luhmer, M.; Constant, J. F.; Defrancq, E.; Dumy, P.; van Dorsselaer, A.; Moucheron, C.; Kirsch-De Mesmaeker, A. *Chem.—Eur. J.* **2005**, *11*, 1507–1517.
(8) Deroo, S.; Le Gac, S.; Ghosh, S.; Villien, M.; Gerbaux, P.; Defrancq, E.; Moucheron, C.; Dumy, P.; Kirsch-De Mesmaeker, A. *Eur. J. Inorg. Chem.* **2009**, 524–532.
(9) Bensasson, R. V.; Salet, C.; Balzani, V. C. R. *Physique* **1979**, *289*, 41–43.
(10) Orellana, G.; Braun, A. M. *J. Photochem. Photobiol. A—Chem.* **1989**, *48*, 277–289.

 10.1021/ja9024287 CCC: $40.75

Chart 1. Structure and Numbering of the Compounds[a]

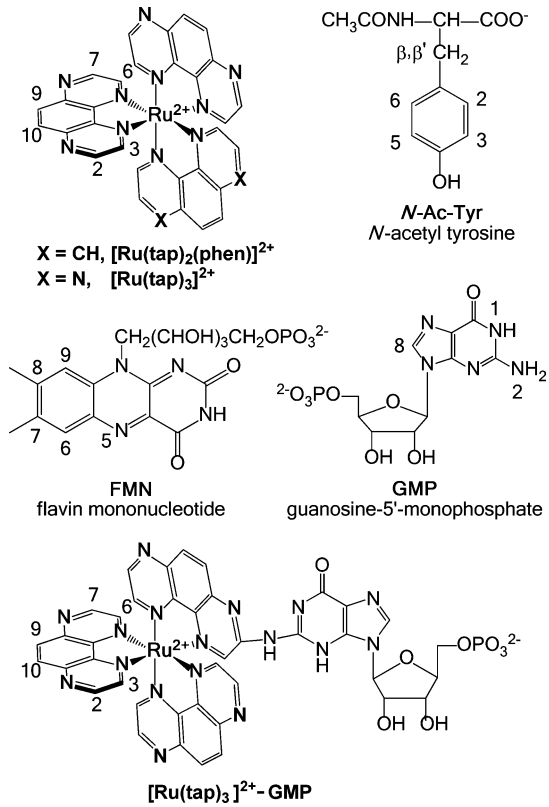

[a] The major forms arising from acid−base equilibria in aqueous solution at pH 7 are represented. The homoleptic $[Ru(phen)_3]^{2+}$ complex (not shown) was also considered. The adduct $[Ru(tap)_3]^{2+}$−GMP was not detected in the present study.

reductive quenching by biomolecules is possible, and direct photoinduced electron transfer from biomolecules to the excited Ru(II) complex has been demonstrated by nano- and picosecond laser flash photolysis.[6,11] These data suggest that photoreactions between polyazaaromatic Ru(II) complexes and biomolecules might give rise to chemically induced dynamic nuclear polarization (CIDNP).

Photo-chemically induced dynamic nuclear polarization (photo-CIDNP) refers to non-Boltzmann nuclear spin state distributions in the products of photochemical reactions and is detected by nuclear magnetic resonance (NMR) spectroscopy as enhanced absorption or emission signals.[12,13] The radical pair mechanism is currently accepted as the most common origin of CIDNP in solution. Accordingly, CIDNP can be observed for those nuclear spins that have a hyperfine interaction with an unpaired electron in transient radical pairs. Therefore, photo-CIDNP can provide valuable information on the transient radicals formed in photoreactions as well as on the photoreaction mechanism. Numerous studies deal with ^{1}H CIDNP originating from photoreactions between flavins or 2,2′-dipyridyl and amino acids, peptides, or proteins.[12,14−20] The photoreaction takes place only if the target, typically the side chain of an aromatic residue, is physically accessible to the photosensitizer. Therefore, photo-CIDNP has been used to probe the surface structure of proteins, to study protein folding, and to investigate recognition processes.[12,14,15,20] Photo-CIDNP has also proved useful for elucidating structural features of double-stranded oligonucleotides and investigating their interactions with drugs.[21−23] Further applications of photo-CIDNP spectroscopy are discussed in a recent authoritative review.[24]

To the best of our knowledge, CIDNP arising from photooxidation of biomolecules by polyazaaromatic Ru(II) complexes has never been reported. Photo-CIDNP could be highly informative regarding the photoreaction of these complexes, allowing one to characterize the transient mono-reduced radicals generated in the radical pair and to identify the potential site(s) of photoaddition between the Ru compound and the biomolecule, with the atomic resolution of ^{1}H NMR spectroscopy. As the first stage of this research, in this work we report results of steady-state ^{1}H photo-CIDNP experiments conducted in deoxygenated (buffered pH 7) aqueous solutions of $[Ru(phen)_3]^{2+}$, $[Ru(tap)_2(phen)]^{2+}$,and $[Ru(tap)_3]^{2+}$ (phen = 1,10-phenanthroline) in the presence of guanosine-5′-monophosphate (GMP) or *N*-acetyltyrosine (*N*-Ac-Tyr). For comparison, experiments were also carried out using flavin mononucleotide (FMN) as photosensitizer.

Materials and Methods

$[Ru(tap)_2(phen)]Cl_2$ and $Ru(tap)_3Cl_2$ were synthesized as previously described.[25,26] $Ru(phen)_3Cl_2$, FMN sodium salt, *N*-acetyl-L-tyrosine, disodium 5′-GMP, and 1,4-dioxane were purchased from Sigma-Aldrich and used as received. A 100 mM phosphate buffer was prepared in D_2O using D_3PO_4 (Isotec) and NaOD (Sigma) to reach pH 7 (uncorrected for deuterium isotope effect).

Luminescence lifetime measurements were conducted at pH 7 and room temperature in aqueous (D_2O) solutions. The samples, ∼0.01 mM Ru(II) complex, 10 mM phosphate, and 150 mM NaCl, were irradiated in a rectangular cell (1 cm × 2 mm) with a frequency-tripled Nd:YAG pulsed laser (Continuum NY 61-10) at 355 nm with an energy of 10 mJ/pulse (pulse width ∼9 ns). The monitoring system includes a monochromator/spectrograph (Acton Research Corp., Spectra Pro 2300i) coupled to a photomultiplier (Hamamatsu R-928) and an oscilloscope (HP 54200A) interfaced

(11) Elias, B.; Creely, C.; Doorley, G. W.; Feeney, M. M.; Moucheron, C.; Kirsch-De Mesmaeker, A.; Dyer, J.; Grills, D. C.; George, M. W.; Matousek, P.; Parker, A. W.; Towrie, M.; Kelly, J. M. *Chem.−Eur. J.* **2008**, *14*, 369–375.
(12) Kaptein, R. Photo-CIDNP Studies of Proteins. In *Biological Magnetic Resonance*; Berliner, L. J., Reubens, J., Eds.; Plenum Press: New York, 1982; Vol. 4, pp 145−191.
(13) Roth, H. D. *J. Photochem. Photobiol. C* **2001**, *2*, 93–116.
(14) Kaptein, R.; Dijkstra, K.; Nicolay, K. *Nature* **1978**, *274*, 293–294.
(15) Hore, P. J.; Winder, S. L.; Roberts, C. H.; Dobson, C. M. *J. Am. Chem. Soc.* **1997**, *119*, 5049–5050.
(16) Tsentalovich, Y. P.; Lopez, J. J.; Hore, P. J.; Sagdeev, R. Z. *Spectrochim. Acta A* **2002**, *58*, 2043–2050.
(17) Tsentalovich, Y. P.; Morozova, O. B.; Yurkovskaya, A. V.; Hore, P. J. *J. Phys. Chem. A* **1999**, *103*, 5362–5368.
(18) Tsentalovich, Y. P.; Morozova, O. B.; Yurkovskaya, A. V.; Hore, P. J.; Sagdeev, R. Z. *J. Phys. Chem. A* **2000**, *104*, 6912–6916.
(19) Tsentalovich, Y. P.; Morozova, O. B. *J. Photochem. Photobiol. A−Chem.* **2000**, *131*, 33–40.
(20) Morozova, O. B.; Yurkovskaya, A. V.; Tsentalovich, Y. P.; Forbes, M. D. E.; Hore, P. J.; Sagdeev, R. Z. *Mol. Phys.* **2002**, *100*, 1187–1195.
(21) Kaptein, R.; Nicolay, K.; Dijkstra, K. *J. Chem. Soc., Chem. Commun.* **1979**, 1092–1094.
(22) Katahira, M.; Sakaguchikatahira, R.; Hayashi, F.; Uesugi, S.; Kyogoku, Y. *J. Am. Chem. Soc.* **1991**, *113*, 8647–8651.
(23) Katahira, R.; Katahira, M.; Yamashita, Y.; Ogawa, H.; Kyogoku, Y.; Yoshida, M. *Nucleic Acids Res.* **1998**, *26*, 744–755.
(24) Goez, M. Photo-CIDNP Spectroscopy. In *Annual Reports on NMR Spectroscopy*; Webb, G., Ed.; Academic Press: London, 2009; Vol. 66.
(25) Kirsch-De Mesmaeker, A.; Nasielski-Hinkens, R.; Maetens, D.; Pauwels, D.; Nasielski, J. *Inorg. Chem.* **1984**, *23*, 377–379.
(26) Lecomte, J. P.; Kirsch-De Mesmaeker, A.; Demeunynck, M.; Lhomme, J. *J. Chem. Soc., Faraday Trans.* **1993**, *89*, 3261–3269.

to a personal computer. Luminescence decays were averaged over 16 shots and fitted to a single exponential between 0.2 and 1 μs for $[Ru(tap)_3]^{2+}$ and between 0.2 and 2 μs for $[Ru(tap)_2(phen)]^{2+}$.

Unless otherwise stated, the photo-CIDNP experiments were conducted on thoroughly deoxygenated samples at neutral pH. The samples, ~0.1 mM Ru(II) complex or 0.2 mM FMN,[27] ~2 mM biomolecule, 0.2 mM 1,4-dioxane, and 10 mM phosphate were prepared by mixing with D_2O suitable volumes of stock solutions of known concentration. Samples of 0.6 mL were bubbled with argon (Air Liquide, Belgium) for 20 min in a standard 5 mm NMR tube at room temperature prior to careful introduction of the optical fiber and sealing with Parafilm.

^{1}H photo-CIDNP spectra were recorded on a 600 MHz NMR spectrometer (Varian VNMR system) at 298 K. The light source was a continuous-wave argon ion laser (Innova 70C series laser model, Coherent) operating at 488 nm. A mechanical shutter controlled by the spectrometer was employed to produce light pulses of 100 ms duration. The samples were irradiated from above via a 1 mm diameter optical fiber, positioned inside a coaxial insert (Wilmad WGS 5BL) whose tip was about 3 mm above the top of the NMR receiver coil.[28] The actual output power of the laser at 488 nm (~2.6 W) and the output power from the optical fiber within the coaxial insert (~1.2 W) were measured before each series of experiments on a single day; the output power from the optical fiber was found to vary by less than 10%. Unless otherwise stated, the spectra were recorded after four steady-state scans using eight transients and the following pulse sequence: 13.5 s relaxation delay − 1.5 s solvent presaturation − 100 ms delay ("dark" spectra) or 100 ms laser pulse ("light" spectra) − 10 ms delay − 3 μs RF pulse (about 40°) − 1.5 s acquisition time. The spectral width was about 16 ppm, centered at the signal of the solvent (HDO). The processing comprised exponential multiplication of the free induction decay with line broadening (lb) parameter of 1 Hz, zero-filling (spectrum digital resolution of 0.07 Hz/point), and calibration of the chemical shift scale with respect to the signal of internal 1,4-dioxane (3.75 ppm). "Dark" and "light" spectra were recorded alternately with a 5 min delay between a "light" spectrum and the subsequent "dark" spectrum. The photo-CIDNP effects were determined as

$$\frac{L_i - (D_i + D_{i+1})/2}{(D_i + D_{i+1})/2} \times 100\%$$

where L_i is the ^{1}H signal integral measured in the "light" spectrum i, and D_i and D_{i+1} are respectively the corresponding equilibrium signal integrals in the "dark" spectra recorded before and after the "light" spectrum i.

Results

The luminescence lifetimes of $[Ru(tap)_3]^{2+}$ and $[Ru(tap)_2(phen)]^{2+}$ were measured using the same solvent as in the photo-CIDNP experiments (10 mM phosphate, D_2O, pH 7), but the solutions were made in 150 mM NaCl in order to avoid significant variations of the ionic strength for increasing biomolecule concentrations (see Supporting Information). The luminescence lifetimes measured in the absence of biomolecule, τ_0, and the quenching rate constants, k_Q, are given in Table 1. These data can be used to calculate the percentage of luminescence quenching, Φ_Q, according to

$$\Phi_Q = 1 - \frac{\tau}{\tau_0} \quad \text{with} \quad \frac{\tau_0}{\tau} = 1 + k_Q\tau_0[B] \qquad (1)$$

Table 1. Physicochemical Characteristics of the Studied Photoreactions[a]

	GMP	*N*-Ac-Tyr
$[Ru(tap)_2(phen)]^{2+}$ ($\tau_{0,air}$ = 840 ns; $\tau_{0,Ar}$ = 1020 ns)		
$\Delta G°_{ET}$ (eV)	−0.06	−0.28
k_Q (10^9 M^{-1} s^{-1})	0.28 ± 0.04	0.161 ± 0.007
Φ_Q (%)	35 ± 4	28 ± 2
$x_{P^{\bullet-}}$ Φ_Q (%)	1.3	1.1
$[Ru(tap)_3]^{2+}$ (τ_0 = 215 ns)		
$\Delta G°_{ET}$ (eV)	−0.25	−0.47
k_Q (10^9 M^{-1} s^{-1})	1.55 ± 0.07	1.85 ± 0.09
Φ_Q (%)	39 ± 2	49 ± 2
$x_{P^{\bullet-}}$ Φ_Q (%)	7.8	9.8

[a] $\Delta G°_{ET}$ is the free energy change associated with the electron-transfer process. It is estimated according to $\Delta G°_{ET} = E_{ox}(B/B^{\bullet+}) - E_{red}(P^*/P^{\bullet-})$, where $E_{ox}(B/B^{\bullet+})$ is the oxidation potential of the biomolecule in the ground state and $E_{red}(P^*/P^{\bullet-})$ is the reduction potential of the excited photosensitizer, *i.e.*, the reduction potential of the lowest energy ^{3}MLCT excited state of the complex. The $E_{ox}(B/B^{\bullet+})$ values used in the calculation are 1.07 V vs SCE for GMP and 0.85 V vs SCE for *N*-Ac-Tyr in aqueous (H_2O) solution at pH 7.[5,30] The $E_{red}(P^*/P^{\bullet-})$ values are 1.13 V vs SCE for $[Ru(tap)_2(phen)]^{2+}$ and 1.32 V vs SCE for $[Ru(tap)_3]^{2+}$ in acetonitrile.[5] τ_0 is the luminescence lifetime of the lowest energy ^{3}MLCT excited state of the complex in the absence of the biomolecules, and k_Q is the luminescence quenching rate constant measured in aerated solutions (room temperature, D_2O, 10 mM phosphate, 150 mM NaCl, pH 7). Reported τ_0 data are the averages of at least two independent measurements; the relative error is estimated to be of the order of 10% with $[Ru(tap)_2(phen)]^{2+}$ under argon and 5% otherwise. The τ_0 values measured for $[Ru(tap)_3]^{2+}$ under air and under argon are not significantly different. The errors quoted for k_Q correspond to twice the fitting errors. Φ_Q is the percentage of luminescence quenching calculated using the Stern−Volmer equation (eq 1) at the biomolecule concentration of the photo-CIDNP experiments (1.9 and 2.4 mM for GMP and *N*-Ac-Tyr, respectively). The error on Φ_Q was estimated considering a relative error of 5% in the concentration. $x_{P^{\bullet-}}$ is the mole fraction of undeuterated mono-reduced photosensitizer as defined by eq 2; at neutral pH, it is calculated to be 0.038 and 0.20 for $[Ru(tap)(tap^{\bullet-})(phen)]^+$ and $[Ru(tap)_2(tap^{\bullet-})]^+$, respectively.

where [B] is the molar concentration of the biomolecule. In the experimental conditions of the photo-CIDNP experiments, Φ_Q is calculated to range between ~30 and 50% (Table 1).

^{1}H NMR spectra were recorded under sample illumination for two different types of control samples: (i) the Ru(II) complexes in the absence of the biomolecules and (ii) $[Ru(phen)_3]^{2+}$ in the presence of the biomolecules, for which no CIDNP effect is expected since the ^{3}MLCT excited state of the complex is not sufficiently oxidizing to give rise to a photoinduced electron transfer with the studied biomolecules. No photo-CIDNP was observed for these samples, and no artifact due to sample illumination, such as significant signal broadening or unforeseen signal intensity variation, was detected. The ^{1}H NMR spectra indicate that $[Ru(phen)_3]^{2+}$ and $[Ru(tap)_2(phen)]^{2+}$ are photostable while, in agreement with previous studies, $[Ru(tap)_3]^{2+}$ undergoes degradation ascribed to the loss of a tap ligand (see Supporting Information).[6,29]

In the presence of the biomolecules, no photodegradation of $[Ru(tap)_3]^{2+}$ was detected, which indicates that the reductive quenching of the ^{3}MLCT state competes efficiently with the dechelation process. ^{1}H photo-CIDNP effects were observed with $[Ru(tap)_3]^{2+}$ and $[Ru(tap)_2(phen)]^{2+}$ (see Figures 1 and 2), but, as mentioned above, no significant photo-CIDNP was detected with $[Ru(phen)_3]^{2+}$. This is in agreement with the

(27) The quantum yield of singlet to triplet excited-state intersystem crossing is about 0.5 for FMN (Grodowski, M. S.; Veyret, B.; Weiss, K. *Photochem. Photobiol.* **1977**, *26*, 341–352) and 1 for the complexes. .
(28) Kuprov, I.; Hore, P. J. *J. Magn. Reson.* **2004**, *171*, 171–175.
(29) Lecomte, J. P.; Kirsch-De Mesmaeker, A.; Kelly, J. M. *Bull. Soc. Chim. Belg.* **1994**, *103*, 193–200.
(30) Butler, J.; Land, E. J.; Swallow, A. J.; Prutz, W. A. *J. Phys. Chem.* **1987**, *91*, 3113–3114.

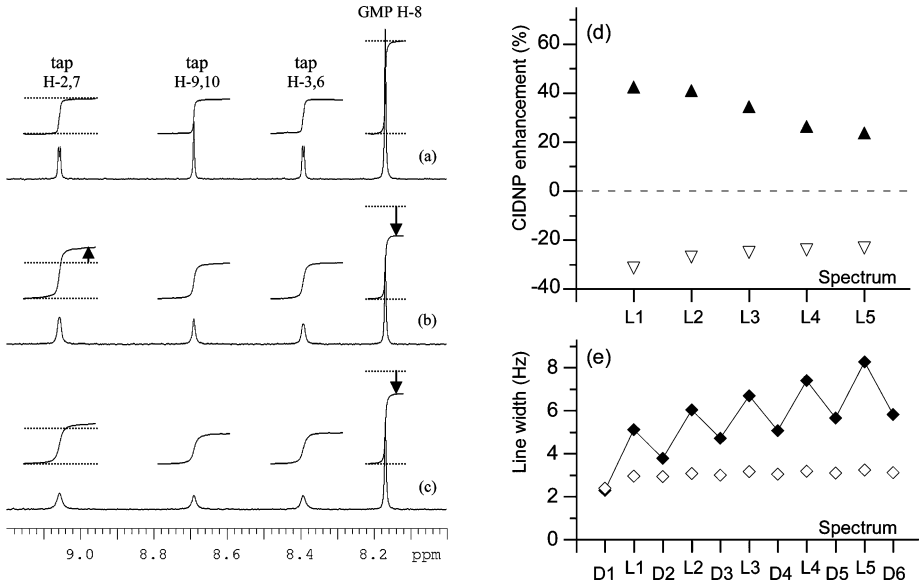

Figure 1. Aromatic regions of 600 MHz ^{1}H NMR spectra, major photo-CIDNP effects, and full line width at half-height for a deoxygenated sample of 1.2×10^{-4} M $[Ru(tap)_3]^{2+}$ and 1.9×10^{-3} M GMP (14.1 T, 298 K, pH 7). D_i and L_i ($i = 1, 2,...$) correspond to successive spectra of eight transients recorded without illumination ("dark" spectra) and with illumination ("light" spectra), respectively. (a) D_1 spectrum: equilibrium spectrum recorded prior to sample illumination. (b) L_1 spectrum: first spectrum recorded with sample illumination. (c) L_5 spectrum: fifth spectrum recorded with sample illumination. (d) Photo-CIDNP effects observed for tap H-2,7 (▲) and GMP H-8 (▽). (e) Line width of the tap H-9,10 (◆) and GMP H-8 (◇) singlet signals (lb = 1.0 Hz).

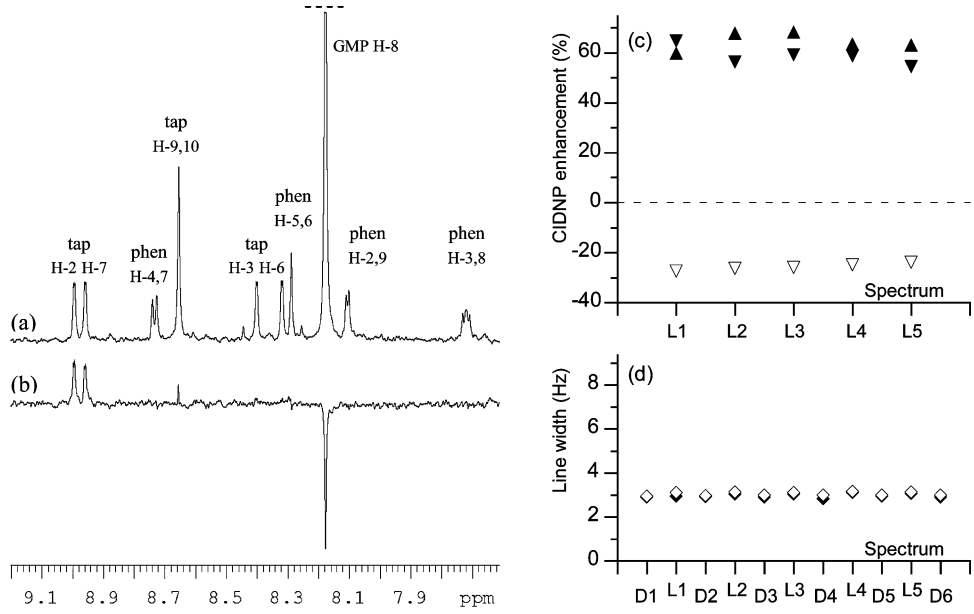

Figure 2. Aromatic regions of 600 MHz ^{1}H NMR spectra, major photo-CIDNP effects, and full line width at half-height for a deoxygenated aqueous solution of 1.1×10^{-4} M $[Ru(tap)_2(phen)]^{2+}$ and 1.8×10^{-3} M GMP (14.1 T, 298 K, pH 7). (a) Equilibrium spectrum recorded prior to sample illumination (D_1 spectrum of eight transients; the signal of GMP-H8 is truncated). (b) Photo-CIDNP difference spectrum: L_1 spectrum (first spectrum recorded with sample illumination, eight transients) minus D_1 spectrum. (c) Photo-CIDNP effects observed for tap H-2 (▲), tap H-7 (▼), and GMP H-8 (▽) in successive "light" spectra. (d) Full line width at half-height of the tap H-9,10 (◆) and GMP H-8 (◇) singlet signals measured in successive "light" and "dark" spectra (lb = 1.0 Hz).

occurrence of a photo-electron-transfer process for those complexes comprising at least two tap ligands. The aromatic regions of ^{1}H NMR spectra recorded for a deoxygenated sample of $[Ru(tap)_3]^{2+}$ and GMP are shown in Figure 1. All of the resonances remain in absorption in the spectra recorded under sample illumination. Clearly, in the first spectrum recorded with illumination (Figure 1b), the integrated intensity of the GMP H-8 signal is decreased compared to that in the equilibrium spectrum (negative photo-CIDNP effect, emissive polarization) while the intensity of the tap H-2,7 signal is increased (positive effect, absorptive polarization). In subsequent spectra recorded under sample illumination, the ^{1}H NMR signals of the complex show marked broadening, while the line width of the GMP signals does not increase significantly, and the photo-CIDNP effects are weaker for both GMP and $[Ru(tap)_3]^{2+}$ (Figure 1c−e). Broadening of the ^{1}H NMR signals of the photosensitizer and concomitant photo-CIDNP extinction were also observed with $[Ru(tap)_3]^{2+}$ in the presence of *N*-Ac-Tyr, as well as with FMN (see Supporting Information). These broadenings persist for hours in thoroughly deoxygenated solutions but vanish instan-

Table 2. Major ^{1}H Photo-CIDNP Enhancements (%) Observed for the Ru(II) Complexes (a) and for GMP and *N*-Ac-Tyr (b)[a]

(a) Ru(II) Complexes

		GMP	*N*-Ac-Tyr
$[Ru(tap)_2(phen)]^{2+}$	tap H-2, H-7	63	43
$[Ru(tap)_3]^{2+}$	tap H-2,7	47	44

(b) GMP and *N*-Ac-Tyr

		$[Ru(tap)_2(phen)]^{2+}$	$[Ru(tap)_3]^{2+}$	FMN
GMP	H-8	−21	−33	232
N-Ac-Tyr	H-3,5	−12	−22	−196 ± 10
	H-2,6	n.s.	n.s.	7
	H-β	10	13	89 ± 8
	H-β'	7	9	58

[a] The data correspond to the average of the photo-CIDNP effects observed at 14.1 T, 298 K, and neutral pH in the first spectrum recorded with illumination for two or three samples. In part a, the estimated absolute error is less than ±10. Unless otherwise indicated, it is less than ±4 in part b. n.s. (not significant) means that the figure is, in absolute value, lower than the estimated error. For $[Ru(tap)_2(phen)]^{2+}$, the photo-CIDNP effects measured for tap H-2 and tap H-7 are not significantly different (see Figure 2c); therefore, the average value is reported. The low- and high-field CH_2 ^{1}H signals of *N*-Ac-Tyr are referred to as H-β and H-β', respectively. Photosensitizer concentration: 1.1×10^{-4} M $[Ru(tap)_2(phen)]^{2+}$; 1.2×10^{-4} M $[Ru(tap)_3]^{2+}$; 2.1×10^{-4} M FMN. Biomolecule concentration: 1.9×10^{-3} M GMP; 2.4×10^{-3} M *N*-Ac-Tyr.

taneously when the solution is brought in contact with air. However, in contrast to FMN (see Supporting Information),[31] no degradation of $[Ru(tap)_3]^{2+}$ was detected in the subsequent ^{1}H NMR spectra. Interestingly, no signal broadening was observed at neutral pH with $[Ru(tap)_2(phen)]^{2+}$. Furthermore, the photo-CIDNP effects remained constant in the successive spectra recorded under illumination (see Figure 2 and Supporting Information).

With both biomolecules studied in this work, ^{1}H photo-CIDNP was observed for the tap ligands, but no significant effect was measured for the phen ligand of $[Ru(tap)_2(phen)]^{2+}$. In the ^{1}H NMR spectrum of $[Ru(tap)_2(phen)]^{2+}$, distinctive signals are observed for tap H-2 and H-7, as well as for tap H-3 and H-6 (see Figure 2a and Supporting Information). For these two pairs of ^{1}H, the measured photo-CIDNP effects are not significantly different (Figure 2c for the tap H-2 and H-7 pair in the presence of GMP). Typically, for both $[Ru(tap)_3]^{2+}$ and $[Ru(tap)_2(phen)]^{2+}$, the magnitude of the detected ^{1}H photo-CIDNP for tap H-3,6 and tap H-9,10 does not exceed ∼15% of the equilibrium polarization at 14.1 T and 298 K (not shown). In contrast, photo-CIDNP effects for tap H-2,7 are significant and are positive. In the first spectrum recorded under illumination, they range from ∼40% to ∼60% (Table 2a).

The photo-CIDNP effects observed for the biomolecules are about 1 order of magnitude weaker with the Ru(II) complexes than with FMN (Table 2b). However, their magnitude is comparable to or larger than typical ^{1}H−^{1}H Overhauser enhancements (NOEs); they are easily detected and can be measured with a good precision.[32] $[Ru(tap)_3]^{2+}$ and

Scheme 1. Processes Involved in Photo-CIDNP[a]

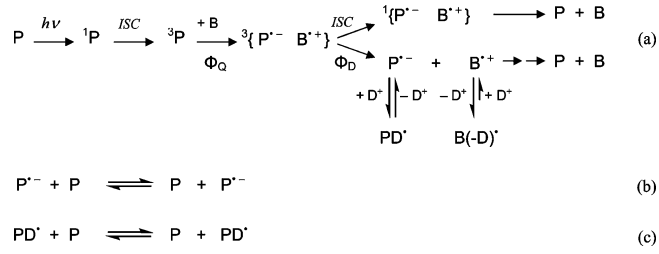

[a] P stands for the photosensitizer and B for the biological target. The processes represented in (a) are photosensitizer excitation, excited triplet-state formation by intersystem crossing, triplet radical pair formation as a consequence of reductive quenching by a biomolecule (Φ_Q is the corresponding quantum yield), intersystem crossing and back electron transfer or radical pair dissociation (Φ_D is the corresponding quantum yield), acid−base equilibria at neutral pH for the free radicals. and recombination of the free radicals. The processes represented in (b) and (c) are, respectively, degenerate electron exchange and degenerate deuterium atom exchange for the photosensitizer (the corresponding exchange reactions for the biomolecule are not shown).

$[Ru(tap)_2(phen)]^{2+}$ give rise to the same pattern of ^{1}H polarization (Table 2b). Moreover, the polarization pattern observed for *N*-Ac-Tyr matches the CIDNP pattern arising from the photoreaction with FMN. However, the photoreaction with the Ru(II) complexes gives rise to emissive GMP H-8 polarization, while absorptive polarization is observed with FMN.

Discussion

The magnitude of photo-CIDNP depends in an intricate way on a number of processes, among which, as shown in Scheme 1 and/or Scheme 2, are photosensitizer excitation, excited triplet-state formation by intersystem crossing, triplet radical pair formation as a consequence of reductive quenching by the biomolecule, intersystem crossing and back electron transfer, radical pair dissociation, paramagnetic relaxation, and recombination of the free radicals as well as acid−base equilibria and degenerate exchange reactions.

The triplet radical pair generated by electron transfer from the biomolecule to the excited photosensitizer (Scheme 2a) is bound to dissociate into free radicals (Scheme 2c) unless a competing process occurs during its lifetime. Typically, such a process consists of intersystem crossing and a subsequent back electron transfer that yields the so-called geminate recombination products, i.e., the diamagnetic parent compounds (Scheme 2b). Intersystem crossing in the radical pair may occur as a consequence of hyperfine interactions between the unpaired electron and a ^{1}H, for instance; this mechanism brings about the nuclear spin-sorting that is the origin of CIDNP. Accordingly, a fraction of the geminate recombination products and the corresponding amount of free radicals, referred to as the escape radicals, are generated with equal but opposite nuclear polarizations (Scheme 2b-2,3 and c-2,3). The spin sorting process is not very efficient, but, because equilibrium nuclear spin-state population differences are weak, it may significantly affect the overall nuclear polarizations. In steady-state photo-CIDNP experiments, the detected polarizations are mainly the result of incomplete cancellation of geminate polarizations by escape polarizations. The geminate polarizations carried by the

(31) The reduced forms $FMND^\bullet$ and $FMND_2$ react with molecular oxygen, and FMN is recovered in this reaction, at least partially (Song, S. H. Dick, B. Penzkofer, A. *Chem. Phys.* **2007**, *332*, 55–65). Indeed, after contact with air, no broadening of the ^{1}H NMR signals of FMN was observed, but the recorded spectra showed additional signals ascribable to irreversible degradation of FMN (see Supporting Information). The reduced forms of the Ru(II) complexes also react with oxygen (see Scheme S1e).

(32) The absolute variation of the ^{1}H NMR signal integral is typically larger for the biomolecules than for the complexes. The corresponding photo-CIDNP effects are weaker for the biomolecules because the equilibrium integrated intensities are larger; the biomolecule concentration is indeed about 1 order of magnitude larger than the Ru(II) complex concentration.

Scheme 2. Origin of the Geminate and Escape Polarizations in Steady-State Photo-CIDNP Experiments[a]

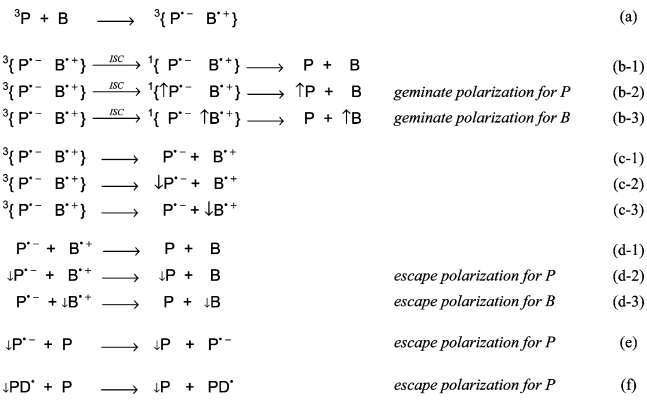

[a] P stands for the photosensitizer and B for the biological target. ^{1}H CIDNP's are indicated by arrows, up meaning absorptive polarization (arbitrarily assigned to geminate recombination products) and down meaning emissive polarization (arbitrarily assigned to escape products); the smaller down arrow indicates reduced emissive polarization as a consequence of paramagnetic relaxation. (a) Triplet radical pair formation due to the reductive quenching of the triplet excited state of the photosensitizer by the biomolecule. (b) Intersystem crossing and back electron transfer: (b-1) without polarization of the parent diamagnetic compounds and (b-2,3) with geminate polarization for the photosensitizer or for the biomolecule. (c-1,2,3) Triplet radical pair dissociation and escape of free radicals in solution. (d) Random encounter and recombination of the free radicals: (d-1) without polarization of the parent diamagnetic compounds and (d-2,3) with escape polarization for the photosensitizer or for the biomolecule. Escape polarization for the photosensitizer arising as a consequence of (e) degenerate electron exchange and (f) degenerate deuterium atom exchange (corresponding (e) and (f) processes for the biomolecule and acid−base equilibria are not represented).

diamagnetic parent compounds build up on the nanosecond time scale or faster (Scheme 2b-2,3). Recombination of the free radicals arises on the microsecond time scale or slower. It yields the diamagnetic parent compounds as well (Scheme 2d), and both the photosensitizer and the biomolecule recovered in this way may carry escape polarizations (Scheme 2d-2,3). In addition, degenerate exchange reactions involving polarized free radicals may also yield the diamagnetic parent compounds with escape polarizations (Scheme 2e and f). The escape polarizations carried by the diamagnetic parent compounds cancel the geminate polarizations, but not completely. Indeed, as a consequence of paramagnetic relaxation in the free radicals, the escape polarizations are significantly reduced and do not balance the geminate polarizations.

The magnitude of steady-state photo-CIDNP effects depends on the percentage of light absorption (Scheme 1a), but, for a given photosensitizer and properly controlled experimental conditions, the amount of excited photosensitizer (^{3}P) generated during sample illumination can be assumed constant, allowing comparisons of photo-CIDNP effects observed with various biomolecules. The quantum yield of triplet radical pair formation, i.e., the ratio between the number of triplet radical pairs and the number of excited photosensitizer molecules, can be estimated as the percentage of luminescence quenching, Φ_Q (Scheme 1a), and calculated using the Stern−Volmer equation (eq 1 and Table 1). Although the reductive quenching of the excited complex by the biomolecule is an essential step for the occurrence of photo-CIDNP, the results do not show a clear-cut correlation between the percentage of luminescence quenching and the magnitude of the photo-CIDNP effect. For $[Ru(tap)_2(phen)]^{2+}$, the calculated Φ_Q value is somewhat larger with GMP than with *N*-Ac-Tyr (Table 1), and the tap H-2,7 photo-CIDNP observed with GMP is also larger than with *N*-Ac-Tyr (Table 2). However, for $[Ru(tap)_3]^{2+}$, the calculated Φ_Q value is significantly smaller with GMP than with *N*-Ac-Tyr, but similar tap H-2,7 photo-CIDNP effects are observed with both biomolecules.

Nuclear spin configuration-dependent intersystem crossing is at the origin of photo-CIDNP (Scheme 2b-2,3) and competes with other possible intersystem crossing mechanisms (Scheme 2b-1). A priori, intersystem crossing due to spin−orbit interaction is expected to be more efficient for triplet radical pairs arising from photoreaction with the complexes, which comprise a heavy Ru atom, than with FMN. Accordingly, weaker photo-CIDNP effects might be expected with the Ru(II) complexes. The magnitude of the photo-CIDNP effects observed for the biomolecules is indeed weaker by about 1 order of magnitude with the Ru(II) complexes than with FMN (Table 2b). However, it must be stressed that various other processes shown in Scheme 2 might explain this observation.

As mentioned above, no significant effect was measured for the phen ligand of $[Ru(tap)_2(phen)]^{2+}$. This is in agreement with the fact that the lowest energy ^{3}MLCT excited states, which are responsible for the photo-oxidation of the biomolecules, correspond to a Ru(II)−tap electronic transition.[4,5] Consequently, in the mono-reduced complex, the unpaired electron is localized on a tap ligand. $[Ru(tap)_3]^{2+}$ and $[Ru(tap)_2(phen)]^{2+}$ are closely related complexes, and the photo-CIDNP results show that, within the short-lived radical pairs, the corresponding mono-reduced radicals have similar properties. Indeed, for each of the biomolecules, both complexes give rise to the same ^{1}H polarization pattern (Table 2b). Furthermore, a unique pattern of photo-CIDNP is observed for both $[Ru(tap)_3]^{2+}$ and $[Ru(tap)_2(phen)]^{2+}$ (i.e., significant absorptive ^{1}H polarization for tap H-2,7 only; Table 2a). This indicates that, at neutral pH, the hyperfine interactions with the various ^{1}H of a tap ligand in the transient radical pairs, and thus the unpaired electron density on that ligand, are highly similar for both complexes and are independent of the biomolecule. In addition, this polarization pattern indicates high unpaired electron density in the vicinity of H-2 and H-7. This agrees with the fact that positions 2 and 7 are more reactive toward photoaddition, as indicated by the structure of the isolated adducts (Chart 1).[33] It is noteworthy that ruthenium complex radicals have proved difficult to detect by time-resolved electron paramagnetic resonance (EPR) spectroscopy, presumably because of the rapid electron spin relaxation.[34,35] The nuclear polarizations of the diamagnetic reaction products, however, are not significantly

(33) The photolysis of $[Ru(tap)_3]^{2+}$ in the presence of GMP yields (i) the major photoadduct $[Ru(tap)_3]^{2+}$-GMP, in which the exocyclic amino group of the guanine nucleobase is covalently linked to C-2 of one of the heterocyclic tap ligands (Jacquet, L. Kelly, J. M. Kirsch-De Mesmaeker, A. *J. Chem. Soc., Chem. Commun.* **1995**, 913–914) and (ii) the binuclear $[Ru(tap)_2(tap\text{-}tap)Ru(tap)_2]^{4+}$ complex formed by the covalent linkage of two tap ligands at C-2 positions (Jacquet, L. Kelly, J. M. Kirsch-De Mesmaeker, A. *Inorg. Chem. Commun.* **1999**, *2*, 135–138). Furthermore, the photoreaction of $[Ru(tap)_2(bpy)]^{2+}$ (bpy = 2,2′-bipyridyl) in the presence of DNA leads to two isomeric covalent adducts involving the N-2 of guanine and the position C-2 or C-7 of one of the tap ligands (Jacquet, L. Davies, R. J. H. Kirsch-De Mesmaeker, A. Kelly, J. M. *J. Am. Chem. Soc.* **1997**, *119*, 11763–11768).

(34) van Slageren, J.; Martino, D. M.; Kleverlaan, C. J.; Bussandri, A. P.; van Willigen, H.; Stufkens, D. J. *J. Phys. Chem. A* **2000**, *104*, 5969–5973.

(35) Concepcion, J. J.; Brennaman, M. K.; Deyton, J. R.; Lebedeva, N. V.; Forbes, M. D. E.; Papanikolas, J. M.; Meyer, T. J. *J. Am. Chem. Soc.* **2007**, *129*, 6968–6969.

affected by electron spin relaxation in the radicals unless it occurs on the time scale (~10 ns) of the geminate radical pair recombination.[36] Photo-CIDNP is thus a powerful method for the magnetic characterization of radicals that are difficult or impossible to detect directly by EPR.[37]

The increasing width of the $[Ru(tap)_3]^{2+}$ signals observed in the ^1H NMR spectra recorded after sample illumination (see data for "dark" spectra in Figure 1e and Supporting Information) indicates the accumulation of long-lived radical species in exchange with the diamagnetic complex. The total amount of free mono-reduced Ru(II) complex radicals generated in solution depends on the photosensitizer excitation, on the quantum yield of triplet radical pair formation (Φ_Q), and on the quantum yield of triplet radical pair dissociation (Φ_D) (Scheme 1a). As suggested by the extinction coefficients,[38] the excitation of $[Ru(tap)_2(phen)]^{2+}$ is expected to be somewhat more efficient than the excitation of $[Ru(tap)_3]^{2+}$. Similar Φ_Q values are estimated for the reductive quenching of the ^{3}MLCT states of both complexes by GMP (35% for $[Ru(tap)_2(phen)]^{2+}$ and 39% for $[Ru(tap)_3]^{2+}$, Table 1). For the system $[Ru(tap)_3]^{2+}$/GMP, Φ_D was measured to be 0.30 (H_2O, 0.1 M phosphate buffer pH 7, Ar-saturated solution),[39] indicating that a significant amount of free radicals may be generated in this photoreaction. Φ_D is not known for the other systems considered in this study. However, since $[Ru(tap)_3]^{2+}$ and $[Ru(tap)_2(phen)]^{2+}$ are closely related complexes, Φ_D is expected to be similar for a given biomolecule. With GMP, the total amount of free radicals generated in solution is thus expected to be similar for both complexes or even somewhat larger for $[Ru(tap)_2(phen)]^{2+}$. Therefore, the fact that line broadening is observed for the ^1H NMR signals of $[Ru(tap)_3]^{2+}$ but not for the signals of $[Ru(tap)_2(phen)]^{2+}$ cannot be simply explained by the total amount of free mono-reduced Ru(II) complex radicals generated in solution. Three processes are likely to cause broadening of the photosensitizer NMR signals: degenerate electron exchange (Scheme 1b), degenerate deuterium atom exchange (Scheme 1c), and/or, by analogy with FMN,[40] bimolecular disproportionation (not shown). In H_2O, the nonchelating nitrogen atoms of $tap^{\bullet-}$ in the reduced complex can be protonated; the pK_a is estimated to be 7.6[41,42] and 8.4[42] for the mono-reduced complex of $[Ru(tap)_3]^{2+}$ and $[Ru(tap)_2(phen)]^{2+}$, respectively. For both species, the major form in D_2O at neutral pH is thus the deuterated mono-reduced complex $PD^{\bullet}$, i.e., $[Ru(tap)_2(tapD^{\bullet})]^{2+}$ and $[Ru(tap)(tapD^{\bullet})(phen)]^{2+}$. However, the mole fraction of the undeuterated mono-reduced complex, $x_P^{\bullet-}$ (eq 2), is significantly higher with $[Ru(tap)_3]^{2+}$ than with $[Ru(tap)_2(phen)]^{2+}$; it is calculated to be ~0.2 and 0.04, respectively.

$$x_P^{\bullet-} \frac{[P^{\bullet-}]}{[P^{\bullet-}] + [PD^{\bullet}]} = \frac{10^{-pK_a}}{10^{-pK_a} + 10^{-pH}} \quad (2)$$

$$\Phi_P^{\bullet-} = x_P^{\bullet-} \Phi_Q \Phi_D \quad (3)$$

Comparison of the quantum yields of undeuterated mono-reduced complex formation, $\Phi_P^{\bullet-}$ as defined by eq 3, is unfortunately not possible because Φ_D is known only for the system $[Ru(tap)_3]^{2+}$/GMP (*vide supra*). The product $x_P^{\bullet-}\Phi_Q$ is nevertheless given in Table 1. With both GMP and *N*-Ac-Tyr, it is significantly larger for $[Ru(tap)_3]^{2+}$ than for $[Ru(tap)_2(phen)]^{2+}$. This suggests that degenerate electron exchange between the diamagnetic complex and the undeuterated radical (Scheme 1b), a process which is expected to be faster than deuterium atom exchange or bimolecular disproportionation, is the primary cause of signal broadening. This is supported by the following additional results of photo-CIDNP experiments in the presence of GMP (not shown): (i) weaker broadening of the ^1H NMR signals of $[Ru(tap)_3]^{2+}$ was observed in acidic conditions, i.e., for a lower mole fraction of the undeuterated radical ($x_P^{\bullet-} < 0.2$), and (ii) broadening of the ^1H NMR signals of $[Ru(tap)_2(phen)]^{2+}$ was observed above pH 7.50 ($x_P^{\bullet-} > 0.1$).

Accumulation of mono-oxidized biomolecule free radicals is concomitant with accumulation of mono-reduced Ru(II) complex free radicals (Schemes 1a and 2c). The absence of significant broadening of the ^1H NMR signals of the biomolecules suggests that no effective electron exchange process takes place, and this agrees with the acid−base properties of the mono-oxidized species.[43] Indeed, the photogenerated oxidized biomolecules studied in this work are deprotonated at pH 7 (Scheme 1a) and can be represented as $B(-D)^{\bullet}$ in D_2O. Degenerate deuterium atom exchange might occur in our experimental conditions but, as in the case of the complexes, does not give rise to significant broadening of the ^1H NMR signals of the biomolecules.

Various processes may be responsible for the photo-CIDNP extinction observed in successive measurements. (i) Accumulation of mono-reduced complexes decreases the actual amount of Ru(II) compound available for photoreaction with the biomolecule. (ii) According to Scheme 2e and f, degenerate exchange reactions may increase the escape polarizations of the complexes, leading to better cancellation of the geminate polarizations and, consequently, weaker photo-CIDNP effects.

(36) Kuprov, I.; Craggs, T. D.; Jackson, S. E.; Hore, P. J. *J. Am. Chem. Soc.* **2007**, *129*, 9004–9013.

(37) Kiryutin, A. S.; Morozova, O. B.; Kuhn, L. T.; Yurkovskaya, A. V.; Hore, P. J. *J. Phys. Chem. B* **2007**, *111*, 11221–11227.

(38) The extinction coefficients of $[Ru(tap)_3]^{2+}$ and $[Ru(tap)_2(phen)]^{2+}$ at 488 nm were measured to be respectively 2.2×10^3 and 7.8×10^3 $M^{-1}cm^{-1}$ at 25 °C in pure water. Using the Beer−Lambert law with a concentration of 1.2×10^{-4} M and an optical path length of 2 cm, the percentage of light absorption in the NMR detection zone is estimated to be 71% and 99%, respectively.

(39) Lecomte, J. P.; Kirsch-De Mesmaeker, A.; Feeney, M. M.; Kelly, J. M. *Inorg. Chem.* **1995**, *34*, 6481–6491.

(40) The photo-induced reduction of the triplet excited state of FMN by a biomolecule yields the flavosemiquinone radical anion, $FMN^{\bullet-}$, and the mono-oxidized radical $B^{\bullet+}$. $FMN^{\bullet-}$ undergoes protonation at pH 7 to form the radical $FMND^{\bullet}$ in D_2O (in H_2O, the pK_a of N-5 in $FMN^{\bullet-}$ is 8.4: Sakai, M. Takahashi, H. *J. Mol. Struct.* **1996**, *379*, 9–18). In the absence of oxygen, the decay of $FMND^{\bullet}$ proceeds by bimolecular recombination with the mono-oxidized biomolecule. $FMND^{\bullet}$ is also involved in a bimolecular disproportionation equilibrium that yields FMN and the fully reduced flavin $FMND_2$ (Song, S. H. Dick, B. Penzkofer, A. *Chem. Phys.* **2007**, *332*, 55–65). The exchange between the radical $FMND^{\bullet}$ and the diamagnetic FMN molecule is thought to be mainly at the origin of the broadening of the ^1H NMR signals of FMN (Maeda, K. Lyon, C. E. Lopez, J. J. Cemazar, M. Dobson, C. M. Hore, P. J. *J. Biomol. NMR* **2000**, *16*, 235–244), although degenerate D exchange between $FMND^{\bullet}$ and FMN might also occur. The occurrence of bimolecular disproportionation has been suggested for Ru(II) complexes (Tan-Sien-Hee, L. Kirsch-De Mesmaeker, A. *J. Chem. Soc., Dalton Trans.* **1994**, *24*, 3651–3658. Neshvad, G. Hoffman, M. Z. Mulazzani, Q. G. Venturi, M. Ciano, M. Dangelantonio, M. *J. Phys. Chem.* **1989**, *93*, 6080–6088).

(41) Lecomte, J. P.; Kirsch-De Mesmaeker, A.; Kelly, J. M.; Tossi, A. B.; Gorner, H. *Photochem. Photobiol.* **1992**, *55*, 681–689.

(42) Boisdenghien, A. Photophysique et photochimie de complexes de Ru(II) en présence d'acides nucléiques, d'acides aminés et des biopolymères correspondants. Ph.D. Thesis, Université Libre de Bruxelles, 2007.

(43) The pK_a of N-1 in $GMP^{\bullet+}$ is 3.9 (Steenken, S. *Chem. Rev.* **1989**, *89*, 503–520), and the pK_a of the hydroxyl group of $Tyr^{\bullet+}$ is 2.2 (Bansal, K. M. Fessenden, R. W. *Radiat. Res.* **1976**, *67*, 1–8).

Similarly, degenerate deuterium atom exchange may cause the photo-CIDNP extinction for the biomolecules. (iii) Recombination of free radicals might also play a significant role. Indeed, the accumulation of the mono-reduced complex speeds up the recombination of the freshly formed mono-oxidized biomolecule free radicals that are carrying escape polarization (Scheme 2d-3). Likewise, accumulation of the mono-oxidized biomolecule speeds up the recombination of the polarized mono-reduced Ru(II) complex free radicals (Scheme 2d-2).[44] Faster recombination decreases the impact of paramagnetic relaxation. Consequently, it increases the magnitude of the escape polarizations carried by the diamagnetic recombination products, leading as well to better cancellation of the geminate polarizations and weaker observed photo-CIDNP. Photo-CIDNP extinction and broadening of the ^{1}H NMR signals of the Ru(II) complexes are found to occur simultaneously. This suggests that effective electron exchange (process (ii), Scheme 2e) is the primary cause of the photo-CIDNP extinction for the complexes. Deuterium atom exchange might contribute to photo-CIDNP extinction for the biomolecules together with process (iii) and possibly process (i).

Conclusion

CIDNP arising from photo-oxidation by polyazaaromatic Ru(II) coordination complexes is reported for the first time and is found to be highly informative. It reveals the unpaired electron density in the transient mono-reduced complex and highlights the potential site(s) of photoaddition with the atomic resolution of ^{1}H NMR spectroscopy. The accumulation of mono-reduced Ru(II) complex free radicals in solution may be responsible for NMR signal broadening and photo-CIDNP extinction, but this can be easily overcome by slightly lowering the pH and might also be avoided by using an oxidant such as H_2O_2 at low concentrations.[45] With $Ru(tap)_2phen^{2+}$, in contrast to experiments carried out with FMN, no photobleaching of the photosensitizer was observed at pH 7, and no significant photo-CIDNP extinction was detected. This is an advantage of this Ru(II) complex for experiments requiring repeated sample illuminations, such as 2D NMR experiments. Although the enhancements observed for the biomolecules are not huge, they are comparable to typical ^{1}H homonuclear NOEs, which are easily detectable, and the lack of photobleaching means that there is no obstacle to extensive signal averaging. Polyazaaromatic Ru(II) complexes are versatile coordination compounds. Indeed, their photoreactivity, size, shape, nuclearity, and consequently their intermolecular interactions with biomolecules can be tuned by changing the nature of the ligands. Obviously, considering the magnitude of the photo-CIDNP enhancements, polyazaaromatic Ru(II) complexes will not supersede traditional photosensitizers such as flavins. However, they might be used in complementary studies and provide a different picture. For instance, being larger than flavins, Ru(II) complexes might be more selective in terms of amino acid side-chain solvent accessibility. Another difference is that mononuclear Ru(II) complexes are twice positively charged, and this might also have an effect, notably with oligonucleotides. The interactions and photochemistry of Ru(II) complexes with oligo- and polynucleotides have been the subject of numerous studies, including studies aimed at investigating the selectivity toward structural characteristics of the double-stranded helix. In contrast, the understanding of their photochemistry with oligopeptides and proteins is still in its infancy. With both oligonucleotides and proteins, identification of the site(s) of photoreaction is difficult to achieve; photo-CIDNP experiments are promising in that respect. In conclusion, the occurrence of photo-CIDNP with polyazaaromatic Ru(II) complexes opens new perspectives, especially for the study of the photochemistry of this type of compound but also for the development of novel photosensitizers that might show higher selectivity toward specific local structures or structural defects of proteins and oligonucleotides.

Acknowledgment. The authors gratefully acknowledge Dr. I. Kuprov and Dr. N. Segebarth for their contribution to the very initial stage of this work, Dr. M. Rebarz for his help in the luminescence lifetime measurements, Dr. F. Pierard for fruitful discussions, and R. D'Orazio for technical support. M.L., A.K., S.P., and E.M. thank the "Communauté française de Belgique" (ARC 2002−2007 no. 286) for financial support. M.L., S.P., and E.M. thank the "Fonds de la Recherche Scientifique" (FNRS-FRS, FRFC 2.4.642.08) and the "Fondation Universitaire David et Alice VAN BUUREN" for financial support.

Supporting Information Available: Scheme showing formation of ^{3}MLCT excited states of Ru(II) polyazaaromatic complexes, reductive quenching, and reactions with molecular oxygen; figures showing luminescence lifetime and corresponding Stern−Volmer plots for $[Ru(tap)_3]^{2+}$ and $[Ru(tap)_2(phen)]^{2+}$ in the presence of GMP and *N*-Ac-Tyr, aromatic region of ^{1}H NMR spectra recorded for a deoxygenated aqueous solution of $[Ru(tap)_3]^{2+}$ in the absence of biomolecules, normalized integrals and line width data for 1,4-dioxane and tap ^{1}H measured for a deoxygenated aqueous solution of $[Ru(tap)_3]^{2+}$ in the absence of biomolecules, major photo-CIDNP effects and full line width at half-height measured in successive spectra for a deoxygenated sample of $[Ru(tap)_3]^{2+}$ and *N*-Ac-Tyr, aromatic region of ^{1}H NMR spectra recorded for a deoxygenated aqueous solution of $[Ru(tap)_2(phen)]^{2+}$ and GMP, major photo-CIDNP effects and full line width at half-height measured in successive spectra for a deoxygenated sample of $[Ru(tap)_2(phen)]^{2+}$ and *N*-Ac-Tyr, regions of ^{1}H NMR spectra recorded for a deoxygenated sample of FMN and GMP, photo-CIDNP effect measured for GMP H-8 in successive spectra for a deoxygenated sample of FMN and GMP, and major photo-CIDNP effects measured for *N*-Ac-Tyr in successive spectra for a deoxygenated sample of FMN and *N*-Ac-Tyr. This material is available free of charge via the Internet at http://pubs.acs.org.

JA9024287

(44) At neutral pH, the bimolecular rate constants of recombination of the radicals $[Ru(tap)_2(tap^{\bullet -})]^+$ and $[Ru(tap)_2(tapH^{\bullet})]^{2+}$ with the mono-oxidized GMP radical are respectively 1.5 and 1.0×10^9 M^{-1} s^{-1} (Lecomte, J. P.; Kirsch-De Mesmaeker, A.; Kelly, J. M.; Tossi, A. B.; Gorner, H. *Photochem. Photobiol.* **1992**, *55*, 681–689). The unprotonated mono-reduced complex recombines somewhat faster owing to its higher reducing power.

(45) Maeda, K.; Lyon, C. E.; Lopez, J. J.; Cemazar, M.; Dobson, C. M.; Hore, P. J. *J. Biomol. NMR* **2000**, *16*, 235–244.